A convenient set of vibrational coordinates for 2D calculation of the tunneling splittings of the ground state and some excited vibrational states for the inversion motion in H_3O^+, H_3O^-, and H_3O•

George A. Pitsevich [a,*], Alex E. Malevich [b], Alexander A. Kamnev [c,*]

[a] *Department of Physical Optics and Applied Informatics, Faculty of Physics, Belarusian State University, Nezavisimosti Ave., 4, 220030, Minsk, Belarus*

[b] *Department of Differential Equations and System Analysis, Faculty of Mechanics and Mathematics, Belarusian State University, Nezavisimosti Ave., 4, 220030, Minsk, Belarus*

[c] *Laboratory of Biochemistry, Institute of Biochemistry and Physiology of Plants and Microorganisms – Subdivision of the Federal State Budgetary Research Institution Saratov Federal Scientific Center of the Russian Academy of Sciences, Prosp. Entuziastov, 13, 410049, Saratov, Russia*

*Corresponding authors: pitsevich@bsu.by (G.A. Pitsevich); aakamnev@ibppm.ru, a.a.kamnev@mail.ru (A.A. Kamnev)

SUBMITTING AUTHOR: aakamnev@ibppm.ru, a.a.kamnev@mail.ru (A.A. Kamnev)

Abstract

Splitting of the ground state and some excited symmetric bending vibrational states due to inversion tunneling of the oxygen atom in the H_3O^+, H_3O^- ions and in the H_3O• radical are analyzed by numerically solving the vibrational Schrödinger equation of restricted (2D) dimensionality. As two vibrational coordinates, we used 1) the distance of the oxygen atom from the plane of a regular triangle formed by three hydrogen atoms and 2) a symmetry coordinate composed of three distances between chemically non-bonded hydrogen atoms. The kinetic energy operator in this case takes the simplest form. The 2D potential energy surface (PES) in the given coordinates was calculated for H_3O^+ at the CCSD(T)/aug-cc-pVTZ and CCSD(T)-F12/cc-pVTZ-F12 levels of theory. The same 2D PES for the H_3O^- anion and H_3O• radical were calculated at the CCSD(T)/aug-cc-pVQZ, CCSD(T)/d-aug-cc-pVQZ and UCCSD(T)/aug-cc-pVQZ, UCCSD(T)/d-aug-cc-pVQZ levels of theory, respectively. The tunneling splittings were calculated for the cations $H_3{}^{16}O^+$, $D_3{}^{16}O^+$, $T_3{}^{16}O^+$, $H_3{}^{18}O^+$, $D_3{}^{18}O^+$, $T_3{}^{18}O^+$. The tunneling splittings for the H_3O^-, D_3O^-, T_3O^- anions and H_3O•, D_3O•, T_3O• radicals were calculated for the first time. The results of calculations demonstrate good agreement with experimental values of the tunneling splittings in the ground state and in some excited vibrational states of the $H_3{}^{16}O^+$ and $D_3{}^{16}O^+$ cations.

KEYWORDS: tunneling, potential barriers; hydronium cation, H_3O^+; H_3O^- anion; H_3O• radical; PES; DVR; explicitly correlated methods

1. INTRODUCTION

The hydronium cation (H_3O^+) is a very interesting object that plays a decisive role in the processes of proton transfer and ionic recombination in the aquatic environment [1, 2] and in biological systems [3], as well as in photochemical processes occurring in the Earth's ionosphere [4, 5], at the interface of air and water–acid media [6], or near the interface of water microdroplets [7]. The interest of astrophysicists in the hydronium cation (HC) is due to its presence in dense interstellar dust clouds and comets [8–16]. Possessing a pyramidal structure in the equilibrium state, HC (like the ammonia molecule) can be realized in the form of two equivalent, mirror-symmetric configurations. In this case, the hydrogen atoms tunnel through the low potential barrier in the planar configuration at a very high frequency of 55.35 cm^{-1} [17,18]. Future precision measurements of this frequency in interstellar space and in laboratories may even be able to inform the nature of dark energy [19,20].

Attempts to theoretically calculate the frequencies of inversion tunneling in HC in the ground and excited vibrational states were made both before [21–26] and after their experimental determination [27–42]. A significant scatter in the values of the calculated tunneling splitting of the oxygen atom in the ground vibrational state (28–83 cm^{-1}) showed that this problem turned out to be a difficult touchstone for various theoretical models used in those works. We note a very good result (51 cm^{-1}) obtained by Shida *et al.* [25] even before the experimental determination of the tunneling splitting in the ground state. Later, very good results on the tunneling splittings both in the ground state and in the excited vibrational states of HC were obtained by Bowman *et al.* [30,34,37]. Even closer to the experimental data were the results of calculations of the energies of the excited vibrational states of HC obtained by Halonen *et al.* [33,35,39]. An analysis of the theoretical works presented in the literature shows that the valence coordinates of O–H bonds and valence angles of H–O–H, or their symmetrized combinations, were most often used as vibrational coordinates to describe the inversion motion of HC in the ground state. In some works, together with the valence coordinates of O–H bonds, the angles between O–H bonds and the plane formed by three hydrogen atoms were used. In [22,23,27,28], in addition to the symmetry coordinates composed of stretching O–H (Q) and bending H–O–H (θ) coordinates, the coordinate h was additionally used which describes the distance from the oxygen atom to the plane of three hydrogen atoms. In [30,34,37], the energies of excited vibrational states were calculated using the MULTIMODE and RVIB4 packages developed by the authors. Later, Neff and Rauhut [42] successfully used normal coordinates for calculating the inversion splittings of the H_3N and H_3O^+

vibrational states. A very sophisticated set of vibrational coordinates was used in [33,35,39]. Despite the significantly complicated derivation of the vibrational Hamiltonian in this case, such a choice of coordinates is fully justified by the high quality of the performed calculations.

Unlike HC, two other very similar compounds (the H_3O• radical (HR) and H_3O^- anion (HA)) have been analyzed by researchers to a much lesser extent. Both species have pyramidal isomers; however, they are not stable at least at room temperature [43–45]. Nevertheless, they can be quite stable at low temperatures and manifest themselves in interstellar space and in comets. The processes of the formation and destruction of HA was studied by Miller [46]. The properties of HR were later analyzed in a number of studies [47–51]. At the same time, as far as we know, there are no data about theoretical or experimental studies of the inversion splitting of the ground or excited vibrational states of HR or HA.

In this work, we propose a convenient set of vibrational coordinates for calculating the tunneling splitting of a Y atom in symmetric molecules, radicals, and ions of the YX_3 type, which are in the ground vibrational state. The two-dimensional set includes the coordinate h which, as before, describes the distance from the Y atom to the plane formed by the X atoms, and the totally symmetric coordinate q^S composed of the distances between the X atoms. Indeed, the process of inversion tunneling in the ground state is most univocally described by the coordinate h, and the probability of the atom Y passing through the potential barrier depends mainly on the lengths of the sides of a regular triangle X_3.

Note that in the molecular symmetry group $D_{3H}(M)$ for those configurations which have the symmetry not lower than the C_{3V} point group, the coordinate symmetry species are as follows: $h^{A_2''}$, $q^{A_1'}$, $Q^{A_1'}$, $\theta^{A_1'}$ [20]. In this case, the following expressions are valid: $\left|h^{A_2''}\right| = \left|h^{A_2''}\left(Q^{A_1'}, \theta^{A_1'}\right)\right|$; $q^{A_1'} = q^{A_1'}\left(Q^{A_1'}, \theta^{A_1'}\right)$;. It is also evident that this choice of coordinates (h, q) greatly simplifies the form of the kinetic energy operator in the 2D Schrödinger equation due to the absence of a mixed derivative.

2. CALCULATION DETAILS

As noted above, the coordinate h transforms according to the A_2'' symmetry species in the molecular symmetry group $D_{3H}(M)$. This means that this coordinate determines not the distance from the oxygen atom to the H_3 plane (in this case it would transform according to the A_1' symmetry species), but the position of the oxygen atom relative to the H_3 plane. In Fig. 1, two equivalent equilibrium configurations of HC are shown. Pyramidal isomers of HR and HA have similar configurations. The coordinate h coincides with the C_3 symmetry axis, its origin is aligned

in the center of the regular triangle $H_1H_2H_3$, and its positive direction is determined by the gimlet rule when the triangle $H_1H_2H_3$ rotates from the H_1 atom to the H_2 atom, etc. Since the direction of h does not change during tunneling, the coordinate of the oxygen atom after tunneling changes its sign to the opposite. In this case, from symmetry considerations, for the potential energy the following is true:

$$U\left(h, q^{A_1'}\right) = U\left(-h, q^{A_1'}\right). \qquad (1)$$

The coordinate $q^{A_1'}$ is defined as a fully symmetrical coordinate:

$$q^{A_1'} = \frac{1}{\sqrt{3}}\left(q_{12} + q_{23} + q_{13}\right); \qquad (2)$$

where q_{ij} have the meaning of ordinary valence coordinates for chemicaly non-bonded atoms H_i and H_j. For the convenience of setting the coordinates h and q ($h \equiv h^{A_2''}$; $q \equiv q^{A_1'}$), when calculating the 2D potential energy surface (PES) using the ORCA 5.0.0 package [52], two dummy atoms (DA_1 and DA_3) were additionally introduced, as shown in Fig. 2. The coordinate h was set as the distance between DA_1 and the O_3 oxygen atom. The q_{ij} values were set using the coordinate l which determines the distance from the H_i atoms to DA_1. At the same time, the coordinates q and l are correlated by the expression $q_{ij} = \sqrt{3}l;$.

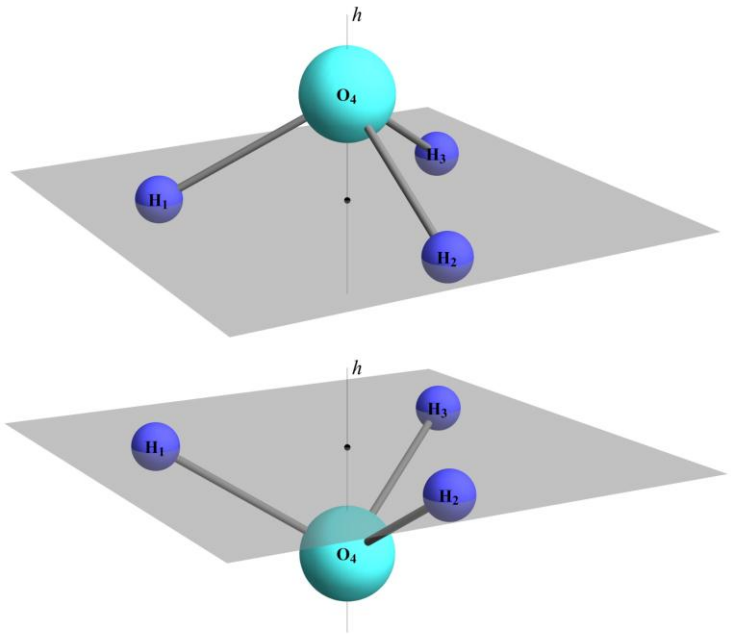

Fig. 1. Two equivalent equilibrium configurations of the hydronium cation passing into each other when the oxygen atom ‘passes’ through the plane of the three hydrogen atoms.

The dummy atom DA_3 was used to ensure that 1) the atoms H_4, H_5, and H_6 formed a regular triangle, 2) the dummy atom DA_1 was in the center of the triangle $H_4H_5H_6$, 3) the atoms O_2, DA_1,

and DA_3 lay on the C_3 symmetry axis. Taking into account expression (1), the calculations were performed for the values $h \geq 0$. The value of the coordinate h was varied in the range $0 \leq h \leq 0.6$ Å for HC and in the range $0 \leq h \leq 0.75$ for HR and HA with a step of 0.05 Å. The coordinate value q was varied in the range $-0.6 \leq q \leq 0.35$ Å with a step of 0.05 Å. The zero value of q was determined in the flat configurations of HC, HA, and HR optimized at the levels of theory used. In this case, the equilibrium values of the distances between hydrogen atoms in this configuration will be denoted as q_{eij}. Then the equilibrium value of the symmetry coordinate can be determined using equation (2) by adding a lower index *e*.

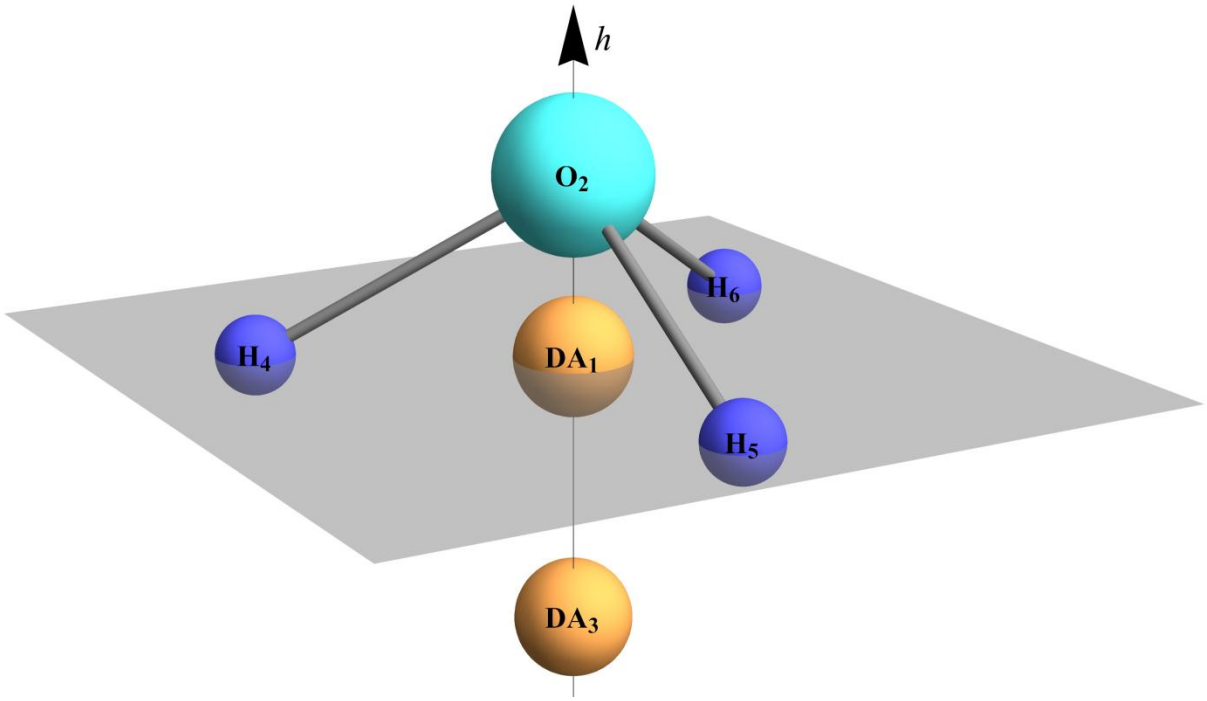

Fig. 2. The arrangement of two dummy atoms (DA_1 and DA_3) in relation to the atomic configuration of the hydronium cation.

Calculations of the 2D PES for HC were performed at two levels of theory: 1) the *ab initio* method CCSD(T) [53–56] in combination with the aug-cc-pVQZ basis set [57–59] and 2) the explicitly correlated *ab initio* method RI-CCSD(T)-F12 [60] in combination with the cc-pVTZ-F12 basis set [61] which was supplemented by the near-complete auxiliary basis set cc-pVTZ-F12-CABS [62,63]. Also, since the calculations used the resolution identity (RI) approximation in combination with the F12 method, then, in accordance with the recommendations from [52], the third basis set cc-pVQZ/C was used. Comparison of the calculation results obtained at these two levels of theory in the analysis of large-amplitude vibrations is of undoubted interest (see [64] and references therein). It was also decided not to take into account the energy of zero-point vibrations [65]. Calculations of the 2D PES for the HR and HA were performed at UCCSD(T)/d-aug-cc-

pVQZ [66], UCCSD(T)/aug-cc-pVQZ, and CCSD(T)/aug-cc-pVQZ, CCSD(T)/d-aug-cc-pVQZ [66] levels of theory, respectively.

The vibrational Schrödinger equation of restricted dimensionality in dimensionless coordinates H, Q, where $H = h / l_0; \quad Q = q / l_0; \quad l_0 = 1Å;$ takes the following form [67,68]:

$$-F_Q(Q)\frac{\partial \Psi}{\partial Q} - F_{QQ}\frac{\partial^2 \Psi}{\partial Q^2} - F_{HH}\frac{\partial^2 \Psi}{\partial H^2} + U(Q,H)\Psi = E\Psi \ , \qquad (3)$$

where: $F_Q(Q) = \frac{\hbar^2}{m_H (Q_e + Q) l_0^2}; \ F_{QQ} = \frac{3\hbar^2}{2 m_H l_0^2}; \ F_{HH} = \frac{(m_O + 3m_H)}{6 m_O m_H l_0^2}; \ Q_e = q_e^{A_1'} / l_0; \quad \hbar$, the Planck constant; m_H, m_O, atomic masses of hydrogen and oxygen, respectively. Equation (3) was solved numerically using the DVR method [69–74]. The elements of the Hamiltonian matrix were calculated using the following formula (4):

$$H_{(i,j)(i'j')} = -F_Q(Q_i) D^Q_{ii'} \delta_{jj'} - F_{QQ} D^{QQ}_{ii'} \delta_{jj'} - F_{HH} \delta_{ii'} D^{HH}_{jj'} + U(Q_i, H_J) \delta_{ii'} \delta_{jj'} \qquad (4)$$

where: $D^{xy} = \tilde{D}^x D^y; \quad D^x_{ii'} = \frac{(-1)^{i'-i}}{2\sin\left[\frac{\pi(i'-i)}{N_x}\right]}; \ D^x_{ii} = 0; \quad i', i \in \{1 \div N_x\}, \ x \in (Q, H), \ N_Q, N_H$ are the numbers of intervals along the coordinates *Q* and *H*, in the center of which the potential energy was calculated. Calculations of the elements of the Hamiltonian matrix and its subsequent diagonalization were carried out using the Mathematica package [75] by analogy with the way it was implemented in [76–78].

3. DISCUSSION OF THE CALCULATION RESULTS

As noted above, the same $|h|$ value corresponds to many values of pairs of coordinates ρ and φ. The same holds for the coordinate q. Therefore, it could be assumed that the stationary vibrational states obtained as a result of solving equation (4) most likely will not be equivalent to the excited states of the symmetric bending vibration of H–O–H angles (ν_2) or to the excited states of the symmetric stretching vibration of O–H bonds (ν_1). Figure 3 shows the 2D PES of HC, HA, and HR.

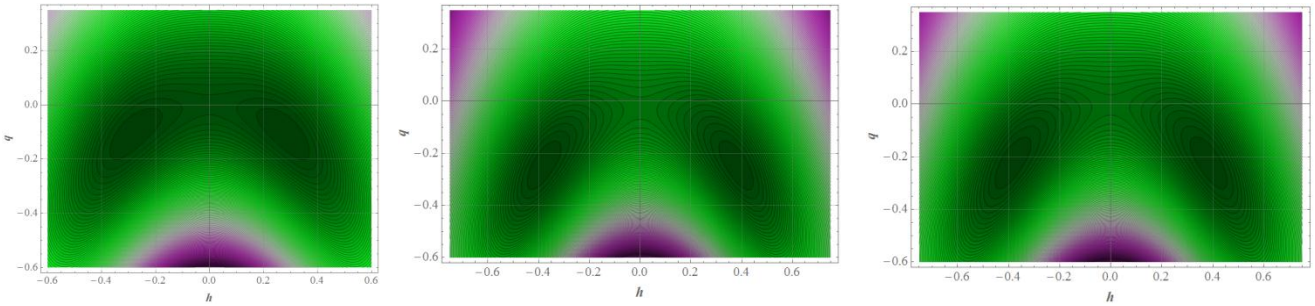

Fig. 3. 2D PES of the HC (left), HA (middle), and HR (right) calculated at the CCSD(T)/aug-cc-pVTZ level of theory.

Figure 3 clearly shows the asymmetry of the potential energy surfaces with respect to the coordinate q and their symmetry with respect to the plane normal to the coordinate plane and intersecting it along the coordinate $h = 0$. The 2D PESs of HR and HA are very similar. In particular, the positions of the minima in both cases are characterized by the values of the coordinates $h = \pm 0.4;\ q = -0.25$. The potential barrier heights for $h = 0$ are 1480 and 1425 cm^{-1} for HR and HA, respectively. The barrier half-widths in both cases are 0.45 Å. In the case of HC, the situation is different. The position of the minimum is characterized by the values of the coordinates $h = \pm 0.3;\ q = -0.1,$ while the height and half-width of the potential barrier for $h = 0$ are 705 cm^{-1} and 0.3 Å. All these data indicate that tunneling in HR and HA should be characterized by lower frequencies than in HC. Table 1 presents the results of calculations of the parameters of equilibrium configurations and the values of the rotational constants for HC, HR, and HA. Table 2 shows the vibration frequencies for HC, HR, and HA calculated in the harmonic approximation at the CCSD(T)/aug-cc-pVQZ level of theory.

Table 1. Geometrical parameters of equilibrium configurations and values of the rotational constants for HC, HR, and HA calculated at the CCSD(T)/aug-cc-pVQZ level of theory.

Compound	l_{O-H} [Å]	φ_{H-O-H} [deg]	B [cm^{-1}]	C [cm^{-1}]
HC	0.9771	111.738	11.031	6.3930
HA	1.0285	106.197	9.5796	6.1823
HR	1.0188	106.295	9.7691	6.2922

Table 2. Vibration frequencies (cm^{-1}) for HC, HR, and HA calculated at the CCSD(T)/aug-cc-pVQZ level of theory.

Compound	$\nu_1(A_1)$	$\nu_2(A_1)$	$\nu_3(E)$	$\nu_4(E)$
HC	3601	899	3700	1699
HA	2798	897	2514	1364
HR	2942	899	2438	1392

According to the data in Tables 1 and 2, the geometric and spectral parameters for HR and HA also turned out to be very similar and differ significantly from the corresponding values for HC.

Table 3 summarizes the energies of the ground and some excited vibrational states ν_2 and ν_1 of the $H_3{}^{16}O^+$ cation calculated in this work, as well as some literature and experimental data. The corresponding data for the $D_3{}^{16}O^+$ and $T_3{}^{16}O^+$ cations are listed in the Supplementary Materials (Tables 1SM and 2SM). Table 4 contains the energies of the ground and some exited vibrational states ν_2 and ν_1 calculated for the first time for the $H_3{}^{16}O$•, $D_3{}^{16}O$•, $T_3{}^{16}O$• radicals and $H_3{}^{16}O^-$, $D_3{}^{16}O^-$, $T_3{}^{16}O^-$ anions at the UCCSD(T)/d-aug-cc-pVQZ, UCCSD(T)/aug-cc-pVQZ, and CCSD(T)/aug-cc-pVQZ, CCSD(T)/d-aug-cc-pVQZ levels of theory, respectively.

Table 3. Energies of excited vibrational states and tunneling splittings for modes ν_2 and ν_1 of the $H_3{}^{16}O^+$ cation calculated at the CCSD(T)/aug-cc-pVQZ and CCSD(T)-F12/cc-pVTZ-F12 levels of theory. The results of similar calculations obtained in [30] and [33] as well as experimental data presented in the literature are also listed.

Vibr. modes	$H_3{}^{16}O^+$									
	E_N (cm^{-1}) CCSD(T)/ aug-cc-pVQZ	E_N (cm^{-1}) CCSD(T)-F12	E_N (cm^{-1}) [30]	E_N (cm^{-1}) [33]	E_{Nexp} (cm^{-1}) [17, 79–81]	$\Delta\nu$ (cm^{-1}) CCSD(T)/ aug-cc-pVQZ	$\Delta\nu$ (cm^{-1}) CSD(T)-F12	$\Delta\nu$ (cm^{-1}) [30]	$\Delta\nu$ (cm^{-1}) [33]	$\Delta\nu_{exp}$ (cm^{-1}) [17,79–81]
GS(+)	0	0	0	0	0	53.48	54.12	46	56.02	55.35
GS(-)	53.48	54.12	46	56.02	55.35					
$\nu_2(+)$	589.9	586.3	580	582.9	581.2	371.7	376.9	354	374.2	373.2
$\nu_2(-)$	961.6	963.2	934	957.1	954.4					
$2\nu_2(+)$	1485.5	1489.1	1445	1479.8	1475.8	578.7	577.6	560	571.2	-
$2\nu_2(-)$	2064.2	2066.7	2005	2051.0	-					
$3\nu_2(+)$	2678.4	2682.7	-	2674.3	-	701.2	698.2	-	665.0	-
$3\nu_2(-)$	3379.6	3380.9	-	3339.3	-					
$\nu_1(+)$	3570.5	3565.3	3400	3449.7	3445.0	29.4	31.1	37	46.8	46.2
$\nu_1(-)$	3599.9	3596.4	3437	3496.5	3491.2					

Table 4. Values of energies and their tunneling splittings (cm^{-1}) for some vibrational states of the $H_3{}^{16}O$•, $D_3{}^{16}O$•, $T_3{}^{16}O$• radicals and $H_3{}^{16}O^-$, $D_3{}^{16}O^-$, $T_3{}^{16}O^-$ anions calculated at the UCCSD(T)/d-aug-cc-pVQZ (dQ), UCCSD(T)/aug-cc-pVQZ (Q), and CCSD(T)/aug-cc-pVQZ (Q), CCSD(T)/d-aug-cc-pVQZ (dQ) levels of theory, respectively.

Vibr. modes	$H_3{}^{16}O$•		$D_3{}^{16}O$•		$T_3{}^{16}O$•		$H_3{}^{16}O^-$		$D_3{}^{16}O^-$		$T_3{}^{16}O^-$	
	dQ	Q	dQ	Q	dQ	Q	dQ	Q	dQ	Q	dQ	Q
GS(+)	0	0	0	0	0	0	0	0	0	0	0	0
GS(-)	3.53	3.39	0.32	0.3	0.07	0.07	4.08	4.10	0.36	0.37	0.08	0.08
ΔGS	**3.53**	**3.39**	**0.32**	**0.3**	**0.07**	**0.07**	**4.08**	**4.10**	**0.36**	**0.37**	**0.08**	**0.08**
$\nu_2(+)$	696.7	705.5	585.6	591.3	520.4	524.6	686.4	682.1	585.7	581.9	522.5	519.1
$\nu_2(-)$	796.2	802.6	601.9	606.9	524.8	528.8	797.3	792.0	604.3	600.6	527.6	524.3
$\Delta\nu_2$	**99.5**	**97.1**	**16.3**	**15.6**	**4.4**	**4.2**	**110.9**	**109.9**	**18.6**	**18.7**	**5.1**	**5.2**
$2\nu_2(+)$	1252.0	1265.8	1009.8	1021.9	931.2	941.3	1248.4	1243.6	1005.2	999.4	929.7	923.5

$2\nu_2(-)$	1628.3	1643.5	1167.7	1178.3	1005.1	1013.5	1638.3	1632.7	1174.1	1169.2	1010.5	1005.1
$\Delta 2\nu_2$	**376.3**	**377.7**	**157.9**	**156.4**	**73.9**	**72.2**	**389.9**	**389.1**	**168.9**	**169.8**	**80.6**	**81.6**
$3\nu_2(+)$	2107.1	2126.6	1480.1	1494.2	1274.9	1286.8	2122.9	2116.4	1488.9	1483.9	1279.6	1273.2
$3\nu_2(-)$	2621.4	2637.6	1794.9	1811.6	1501.4	1514.0	2661.0	2654.1	1810.9	1805.9	1513.6	1507.8
$\Delta 3\nu_2$	**514.3**	**511.0**	**314.8**	**317.4**	**226.5**	**227.2**	**538.1**	**537.7**	**322.0**	**322.0**	**234.0**	**234.6**
$\nu_1(+)$	2740.0	2702.1	2047.7	2043.1	1704.0	1703.9	2561.2	2477.7	1944.5	1913.9	1624.2	1604.8
$\nu_1(-)$	2749.1	2721.3	2048.8	2044.7	1704.3	1704.3	2554.0	2483.0	1946.0	1916.3	1624.5	1605.3
$\Delta\nu_1$	**9.1**	**19.2**	**1.1**	**1.6**	**0.3**	**0.4**	**7.2**	**5.3**	**1.5**	**2.4**	**0.3**	**0.5**

As follows from the data in Tables 3 and 1SM, the values of the tunneling splittings calculated at both levels of theory for the $H_3{}^{16}O^+$ and $D_3{}^{16}O^+$ cations in the ground state are in good agreement with the experimental data ([17, 79–81] and [27, 82, 83], respectively). A somewhat unexpected but very pleasant bonus turned out to be a very good agreement between the calculated and experimental values of the energies of the excited vibrational states of mode ν_2. The calculated values of the tunneling splittings for the $H_3{}^{16}O^+$ and $D_3{}^{16}O^+$ cations for the first excited state of mode ν_2 (371.7 and 193.2 cm^{-1}) are also in excellent agreement with the experimental values (373.2 and 191.4 cm^{-1}). Analysis of the data in Tables 3 and 4 also shows that the calculation results presented in [33] are even closer to the experimental data. However, it should be noted that the authors of [33] solved the full-dimension (6D) vibrational problem. In addition, the contributions of electrons from the inner shells and relativistic effects were taken into account. All this, of course, requires much higher computational efforts. Indeed, equation (4) has a very simple form and is characterized by 1) the absence of a mixed derivative and 2) constant coefficients at the second derivatives. In addition, setting two variables (h and q) completely sets the geometry of the cations and, therefore, when calculating the potential energy, it is not required to optimize the structures with respect to any geometrical parameters. Thus, our calculations were performed using the SP option, which radically reduces the calculation time. At the same time, it should be recognized that the second set of calculated values of the excited vibrational states does not describe adequately the energies of the excited vibrational states of the ν_1 mode. Thus, here our initial assumptions turned out to be correct, and the q coordinate appeared to be incapable of adequately corresponding to the symmetry coordinate associated with the O-H stretching coordinates.

As follows from the results presented in Table 4, the splittings of the ground and excited vibrational states in HR and HA, as expected, turned out to be significantly smaller than those in HC. At the same time, the closeness of the 2PES values for the radical and anion noted above determines the closeness of the tunneling splitting in the ground and excited vibrational states, although in the case of the anion, as can be seen from the data in Table 4, the splittings of

vibrational states due to tunneling turn out to be 10% to 30% larger than in the radical. It should also be noted that the calculated results significantly depend on the basis set used. In general, a similar picture took place in the case of the results presented in [35], where the calculations were performed at the CCSD(T)/aug-cc-pVTZ and CCSD(T)/aug-cc-pVQZ levels of theory. Since, according to [35], the results calculated at the CCSD(T)/aug-cc-pVQZ level of theory were closer to the experimental data, it may be expected that the results obtained at this level of theory, which are given in Table 4, will also be closer to the experimental values.

Tables 2SM and 3SM present the calculated values of some stationary vibrational states of the $T_3{}^{16}O^+$, $H_3{}^{18}O^+$, $D_3{}^{18}O^+$, and $T_3{}^{18}O^+$ cations. Although there are no experimental data for the $T_3{}^{16}O^+$, $H_3{}^{18}O^+$, $D_3{}^{18}O^+$, and $T_3{}^{18}O^+$ cations analyzed in Tables 2SM and 3SM, it should be noted that there is a good agreement between the calculated results in this work and the results presented in [33] for the energies of the excited states and tunneling splittings in the case of mode ν_2. This is especially true in the case of the $T_3{}^{16}O^+$ cation (see Table 2SM). Table 3SM also presents the results of calculations of the energies of vibrational states and the tunneling splittings for the mode ν_2 in the $D_3{}^{18}O^+$ and $T_3{}^{18}O^+$ cations, for which, to the best of our knowledge, similar calculations have not yet been performed. Basing on the comparisons of the calculated and experimental results for the $H_3{}^{16}O^+$ and $D_3{}^{16}O^+$ cations, it may be reasonably expected that the corresponding calculated values of the characteristics for the $D_3{}^{18}O^+$ and $T_3{}^{18}O^+$ cations will also be close to the experimental values.

4. CONCLUSIONS

In this work, we analyzed the inversion motion with a large amplitude and the energies of the excited vibrational states of the mode ν_2 in the $H_3{}^{16}O$, $D_3{}^{16}O$ and $T_3{}^{16}O$ cations, anions and radicals. A convenient set of two vibrational coordinates, h and q, is proposed describing the distance from the oxygen atom to the plane formed by the hydrogen atom isotopes (h) and a fully symmetrical coordinate composed of the distances between chemically non-bonded atoms (q).

In coordinates h, q, a 2D Hamiltonian is obtained, in which there is no mixed derivative, with constant coefficients at the second derivatives, the physical meaning of which is intuitively clear.

The 2D PES of the hydronium cation was calculated at two levels of theory: CCSD(T)/aug-cc-pVQZ and CCSD(T)-F12/cc-pVTZ-F12. Both approaches showed similar results in estimating the energies of the excited vibrational states of the mode ν_2 and the tunneling splittings in the ground and excited states of the mode ν_2. Comparison of the results obtained with published data has

shown that the calculated values of the tunneling splittings for the ground and excited states of mode ν_2 in the $H_3{}^{16}O^+$ and $D_3{}^{16}O^+$ cations agree very well with the experimental data.

The ener***g***ies of ground and excited states and the tunneling splittings for mode ν_2 in the $H_3{}^{16}O$, $D_3{}^{16}O$, and $T_3{}^{16}O$ anions and radicals, for which there are no such data in the literature, have been calculated at the CCSD(T)/d-aug-cc-pVQZ and UCCSD(T)/aug-cc-pVQZ levels of theory. The calculated tunneling splittings in the ground states of the anion (4.1 cm^{-1}) and radical (3.4 cm^{-1}) turned out to be significantly lower than the tunneling splitting in the ground state of the cation (53.5 cm^{-1}), which is due to a significant increase in the height and half-width of potential barriers to inversion in HA and HR as compared to HC.

Author Contributions

Conceptualization, G.A.P.; software, validation, and formal analysis, G.A.P., A.E.M.; investigation and data curation, G.A.P., A.E.M., A.A.K.; visualization, G.A.P.; writing—original draft preparation, G.A.P.; writing—review and editing, A.A.K.; project administration, G.A.P. All authors have read and agreed to the published version of the manuscript.

Acknowledgments

This study was supported by the Belarusian State Program of Scientific Investigations 2021–2025 “GPNI Convergence-25” (11.11.3). The materials of this work were presented at Colloquium Spectroscopicum Internationale XLII (CSI XLII, Gijón, Spain, 30 May – 3 June 2022). A.A.K. would like to express his personal gratitude to the Chairman, Professor Jose M. Costa-Fernandez (Department of Physical and Analytical Chemistry, University of Oviedo, Spain), for support and excellent organization of the congress.

Declaration of competing interest

The authors declare that they have no known competing financial interests or personal relationships that could have appeared to influence the work reported in this paper.

References

[1] J.A.S. Smith, Nuclear magnetic resonance absorption, Q. Rev. Chem. Soc. 7 (1953) 279-306. https://doi.org/10.1039/QR9530700279

[2] A. Hassanali, M.K. Prakash, H. Eshet, M. Parrinello, On the recombination of hydronium and hydroxide ions in water, Proc. Natl. Acad. Sci. USA, 108 (51) (2011) 20410-20415. https://doi.org/10.1073/pnas.1112486108

[3] M. Eigen, Proton transfer, acid-base catalysis, and enzymatic hydrolysis. Part I: Elementary processes, Angew. Chem. Int. Ed. Engl. 3 (1) (1964) 1-19. https://doi.org/10.1002/anie.196400011

[4] R.S. Narcisi, W. Roth, The formation of cluster ions in laboratory sources and in the ionosphere, Adv. Electron. Electron Phys. 29 (1970) 79-113. https://doi.org/10.1016/S0065-2539(08)61090-2

[5] C.J. Howard, H.W. Rundle, F. Kaufman, Water cluster formation rates of NO^+ in He, Ar, N_2, and O_2 at 296ºK, J. Chem. Phys. 55 (1971) 4772-4776. https://doi.org/10.1063/1.1675576

[6] L.M. Levering, M.R. Sierra-Hernández, H.C. Allen, Observation of hydronium ions at the air–aqueous acid interface: Vibrational spectroscopic studies of aqueous HCl, HBr, and HI, J. Phys. Chem. C 111 (25) (2007) 8814-8826. https://doi.org/10.1021/jp065694y

[7] A.J. Colussi, S. Enami, S. Ishizuka, Hydronium ion acidity above and below the interface of aqueous microdroplets. ACS Earth Space Chem. 5 (9) (2021) 2341-2346. https://doi.org/10.1021/acsearthspacechem.1c00067

[8] E. Herbst, W. Klemperer, The formation and depletion of molecules in dense interstellar clouds, Astrophys. J. 185 (1973) 505-533. https://doi.org/10.1086/152436

[9] T. de Jong, A. Dalgarno, W. Boland, Hydrostatic models of molecular clouds, in: B.H. Andrew, Ed., Interstellar Molecules (Symposium – International Astronomical Union, Vol. 87), Cambridge University Press, Cambridge, 1980, pp. 177-181. https://doi.org/10.1017/S0074180900072491

[10] H. Suzuki, Molecular evolution in interstellar clouds. I: Ion chemistry in dense clouds, Progr. Theoret. Phys. 62 (1979) 936-956. https://doi.org/10.1143/PTP.62.936

[11] S.S. Prasad, W.T. Huntress, Jr., A model for gas phase chemistry in interstellar clouds: I. The basic model, library of chemical reactions, and chemistry among C, N, and O compounds. Astrophys. J., Suppl. Ser. 43 (1980) 1-35. https://doi.org/10.1086/190665

[12] W.W. Duley, D.A. Williams, Interstellar Chemistry. Acad. Press, London, 1984, Chap. 3.

[13] H. Roberts, E. Herbst, The abundance of gaseous H_2O and O_2 in cores of dense interstellar clouds, Astron. Astrophys. 395 (2002) 233-242.

[14] A. Wootten, J.G. Magnum, B.E. Turner, M. Bogey, F. Boulanger, F. Combes, P.J. Encrenaz, M. Gerin, Detection of interstellar H_3O^+: A confirming line, Astrophys. J. Part 2: Letters, 380 (1991) L79-L83. https://doi.org/10.1086/186178

[15] T.G. Phillips, E.F. van Dishoeck, J. Keene, Interstellar H_3O^+ and its relation to the O_2 and H_2O abundances, Astrophys. J. 399 (1992) 533-550. https://scholarlypublications.universiteitleiden.nl/access/item%3A2727566/view

[16] E. Iglesias, The chemical evolution of molecular clouds. Astrophys. J., Part 1, 218 (1977) 697-715. https://doi.org/10.1086/155727

[17] D.-J. Liu, T. Oka, Experimental determination of the ground-state inversion splitting in H_3O^+, Phys. Rev. Lett. 54 (1985) 1787-1789. https://doi.org/10.1103/PhysRevLett.54.1787

[18] P. Verhoeve, M. Versluis, J.J. Ter Meulen, W.L. Meerts, A. Dymanus, Far infrared laser sideband spectroscopy of H_3O^+: the pure inversion spectrum around 55 cm^{-1}, Chem. Phys. Lett. 161 (1989) 195-201. https://doi.org/10.1016/S0009-2614(89)87059-9

[19] M.G. Kozlov, S.A. Levshakov, Sensitivity of the H_3O^+ inversion–rotational spectrum to changes in the electron-to-proton mass ratio, Astrophys. J. 726 (2011) 65. https://doi.org/10.1088/0004-637X/726/2/65

[20] A. Owens, S.N. Yurchenko, O.L. Polyansky, R.I. Ovsyannikov, W. Thiel, V. Špirko, Accurate prediction of H_3O^+ and D_3O^+ sensitivity coefficients to probe a variable proton-to-electron mass ratio, Month. Not. R. Astron. Soc. 454 (2015) 2292-2298. https://doi.org/10.1093/mnras/stv2023

[21] G.H.F. Diercksen, W.P. Kraemer, B.O. Roos, SCF-CI studies of correlation effects on hydrogen bonding and ion hydration. The systems: H_2O, $H^+ \cdot H_2O$, $Li^+ \cdot H_2O$, $F^- \cdot H_2O$, and $H_2O \cdot H_2O$, Theoret. Chim. Acta 36 (1975) 249-274. https://doi.org/10.1007/BF00549690

[22] V. Špirko, P.R. Bunker, The inversion potential and rotation-inversion energy levels of H_3O^+ and CH_3^-, J. Mol. Spectrosc. 95 (1982) 226-235. https://doi.org/10.1016/0022-2852(82)90249-1

[23] P.R. Bunker, W.P. Kraemer, V. Špirko, Ab initio rotation-vibration energies of H_3O^+, J. Mol. Spectrosc. 101 (1983) 180-185. https://doi.org/10.1016/0022-2852(83)90015-2

[24] P. Botschwina, P. Rosmus, E.-A. Reinsch, Spectroscopic properties of the hydroxonium ion calculated from SCEP CEPA wavefunctions, Chem. Phys. Lett. 102 (1983) 299-306. https://doi.org/10.1016/0009-2614(83)87045-6

[25] N. Shida, K. Tanaka, K. Ohno, An ab initio calculation of symmetric bending and stretching vibrational states of the H_3O^+ and D_3O^+ ions, Chem. Phys. Lett. 104 (1984) 575-578. https://doi.org/10.1016/0009-2614(84)80030-5

[26] P.R. Bunker, T. Amano, V. Špirko, A preliminary determination of the equilibrium geometry and inversion potential in H_3O^+ from experiment, J. Mol. Spectrosc. 107 (1984) 208-211. https://doi.org/10.1016/0022-2852(84)90277-7

[27] T.J. Sears, P.R. Bunker, P.B. Davies, S.A. Johnson, V. Špirko, Diode laser absorption spectroscopy of D_3O^+: Determination of the equilibrium structure and potential function of the oxonium ion, J. Chem. Phys. 83 (1985) 2676-2685. https://doi.org/10.1063/1.449270

[28] V. Špirko, W.P. Kraemer, Anharmonic potential function and rotation-inversion energy levels of H_3O^+, J. Mol. Spectrosc. 134 (1) (1989) 72-81. https://doi.org/10.1016/0022-2852(89)90129-X

[29] M.A. Gomez, L.R. Pratt, Construction of simulation wave functions for aqueous species: D_3O^+, J. Chem. Phys. 109 (1998) 8783-8789. https://doi.org/10.1063/1.477548

[30] X. Huang, S. Carter, J. Bowman, *Ab initio* potential energy surface and rovibrational energies of H_3O^+ and its isotopomers, J. Chem. Phys. 118 (2003) 5431-5441. https://doi.org/10.1063/1.1555974

[31] F. Dong, D.J. Nesbitt, Jet cooled spectroscopy of H_2DO^+: Barrier heights and isotope-dependent tunneling dynamics from H_3O^+ to D_3O^+, J. Chem. Phys. 125 (2006) 144311. https://doi.org/10.1063/1.2338520

[32] T. Furuya, S. Saito, M. Araki, Microwave spectrum of the H_2DO^+ ion: Inversion-rotation transitions and inversion splitting, J. Chem. Phys. 127 (2007) 244314. https://doi.org/10.1063/1.2813352

[33] T. Rajamäki, A Miani, L. Halonen, Six-dimensional *ab initio* potential energy surfaces for H_3O^+ and NH_3: Approaching the subwave number accuracy for the inversion splittings, J. Chem. Phys. 118 (2003) 10929-10938. https://doi.org/10.1063/1.1574784

[34] X. Huang, S. Carter, J.M. Bowman, Ab initio potential energy surface and vibrational energies of H_3O^+ and its isotopomers, J. Phys. Chem. B 106 (2002) 8182-8188. https://doi.org/10.1021/jp020619i

[35] A. Miani, A. Beddoni, J. Pesonen, L. Halonen, CCSD(T) inversion spectrum for H_3O^+, Chem. Phys. Lett. 363 (2002) 52-56. https://doi.org/10.1016/S0009-2614(02)00964-8

[36] N.J. Wright, R.B. Gerber, Extending the vibrational self-consistent method: Using a partially separable wave function for calculating anharmonic vibrational states of polyatomic molecules, J. Chem. Phys. 114 (2001) 8763-8768. https://doi.org/10.1063/1.1357439

[37] J.M. Bowman, X. Huang, S. Carter, Full dimensional calculations of vibrational energies of H_3O^+ and D_3O^+, Spectrochim. Acta Part A, 58 (2002) 839-848. https://doi.org/10.1016/S1386-1425(01)00672-2

[38] S.N. Yurchenko, J. Tennyson, S. Miller, V.V. Melnikov, J. O'Donoghue, L. Moore, ExoMol line lists – XL. Ro-vibrational molecular line list for the hydronium ion (H_3O^+), Month. Not. R. Astron. Soc. 497 (2020) 2340-2351. https://doi.org/10.1093/mnras/staa2034

[39] T. Rajamäki, J. Noga, P. Valiron, L. Halonen, Inversion levels of H_3O^+ as a probe for the basis set convergence in traditional and explicitly correlated coupled-cluster calculations, Mol. Phys. 102 (2004) 2259-2268. https://doi.org/10.1080/00268970412331287197

[40] D.-J. Liu, T. Oka, T.J. Sears, Calculated ν_2 (inversion) spectrum of H_3O^+, J. Chem. Phys. 84 (1986) 1312-1316. https://doi.org/10.1063/1.450522

[41] S.N. Yurchenko, P.R. Bunker, P. Jensen, Coulomb explosion imaging: the CH_3^+ and H_3O^+ molecules, J. Mol. Struct. 742 (2005) 43-48. https://doi.org/10.1016/j.molstruc.2004.11.092

[42] M. Neff, G. Rauhut, Towards black-box calculations of tunneling splittings obtained from vibrational structure methods based on normal coordinates, Spectrochim. Acta Part A, 119 (2014)

100-106. https://doi.org/10.1016/j.saa.2013.02.033

[43] W.J. Griffiths, F.M. Harris, Energetics of charge-inversion reactions of H_3O^+ and H_3O^- ions, Int. J. Mass Spectrom. Ion Proc., 77 (1987) R7-R12. https://doi.org/10.1016/0168-1176(87)87013-1

[44] J.V. Ortiz, Ionization energies of OH_3^- isomers, J. Chem. Phys. 91 (1989) 7024-7029. https://doi.org/10.1063/1.457319

[45] M. Gutowski, J. Simons, Double-Rydberg anions: Ground-state electronic and geometric stabilities, J. Chem. Phys. 93 (1990) 3874-3880. https://doi.org/10.1063/1.458773

[46] T.M. Miller, A.A. Viggiano, A. E. Stevens Miller, R.A. Morris, M. Henchman, J.F. Paulson, J.M. Van Doren, The formation and destruction of H_3O^-, J. Chem. Phys. 100 (1994) 5706-5714. https://doi.org/10.1063/1.467136

[47] M. Luo, M. Jungen, The H_3O Rydberg radical, Chem. Phys. 241 (1999) 297-303. https://doi.org/10.1016/S0301-0104(98)00426-1

[48] J.K. Park, B.G. Kim, I.S. Koo, Avoided curve crossings for the dissociation of the Rydberg H_3O radical into ($OH+H_2$), Chem. Phys. Lett., 356 (2002) 63-72. https://doi.org/10.1016/S0009-2614(02)00308-1

[49] M. Ončák, P. Slaviček, M. Fárnik, U. Buck, Photochemistry of hydrogen halides on water clusters: Simulations of electronic spectra and photodynamics, and comparison with photodissociation experiments, J. Phys. Chem. A 115 (2011) 6155-6168. https://doi.org/10.1021/jp111264e

[50] F. Uhlig, O. Marsalek, P. Jungwirth, From a localized H_3O radical to a delocalized $H_3O^+\cdots e^-$ solvent-separated pair by sequent hydration. Phys. Chem. Chem. Phys. 13 (2011) 14003-14009. https://doi.org/10.1039/C1CP20764D

[51] F.J. Hernández, M.C. Capello, A. Naito, S. Manita, K. Tsukada, M. Miyazaki, M. Fujii, M. Broquier, G. Gregoire, C. Dedonder-Lardeux, C. Jouvet, G.A. Pino, Trapped hydronium radical produced by ultraviolet excitation of substituted aromatic molecule, J. Phys. Chem. A 119 (2015) 12730-12735. https://doi.org/10.1021/acs.jpca.5b10142

[52] F. Neese, F. Wennmohs, U. Becker, C. Riplinger, The ORCA quantum chemistry program package, J. Chem. Phys. 152 (2020) 224108. https://doi.org/10.1063/5.0004608

[53] K. Raghavachari, G.W. Trucks, J.A. Pople, M. Head-Gordon, A fifth-order perturbation comparison of electron correlation theories, Chem. Phys. Lett. 157 (1989) 479-483. https://doi.org/10.1016/S0009-2614(89)87395-6

[54] C. Hampel, H.-J. Werner, Local treatment of electron correlation in coupled cluster theory, J. Chem. Phys. 104 (1996) 6286-6297. https://doi.org/10.1063/1.471289

[55] M. Schütz, Low-order scaling local electron correlation methods. III. Linear scaling local perturbative triples correlation (*T*), J. Chem. Phys. 113 (2000) 9986-10001. https://doi.org/10.1063/1.1323265

[56] M. Schütz, H.-J. Werner, Local perturbative triplets correction (T) with linear cost scaling, Chem. Phys. Lett., 318 (2000) 370-378. https://doi.org/10.1016/S0009-2614(00)00066-X

[57] K.A. Peterson, D.E. Woon, T.H. Dunning, Jr., Benchmark calculations with correlated molecular wave functions. IV. The classical barrier height of the $H+H_2 \rightarrow H_2+H$ reaction, J. Chem. Phys. 100 (1994) 7410-7415. https://doi.org/10.1063/1.466884

[58] A.K. Wilson, T. van Mourik, T.H. Dunning, Jr., Gaussian basis sets for use in correlated molecular calculations. VI. Sextuple zeta correlation consistent basis sets for boron through neon, J. Mol. Struct. THEOCHEM 388 (1996) 339-349. https://doi.org/10.1016/S0166-1280(96)80048-0

[59] R.A. Kendall, T.H. Dunning, Jr., R.J. Harrison, Electron affinities of the first-row atoms revisited. Systematic basis sets and wave functions, J. Chem. Phys. 96 (1992) 6796-6806. https://doi.org/10.1063/1.462569

[60] H.-J. Werner, T.B. Adler, F.R. Manby, General orbital invariant MP2-F12 theory, J. Chem. Phys. 126 (2007) 164102. https://doi.org/10.1063/1.2712434

[61] K.A. Peterson, T.B. Adler, H.-J. Werner, Systematically convergent basis sets for explicitly correlated wavefunctions: The atoms H, He, B–Ne, and Al–Ar, J. Chem. Phys. 128 (2008) 084102. https://doi.org/10.1063/1.2831537

[62] T.B. Adler, G. Knizia, H.-J. Werner, A simple and efficient CCSD(T)-F12 approximation, J. Chem. Phys. 127 (2007) 221106. https://doi.org/10.1063/1.2817618

[63] K.E. Yousaf, K.A. Peterson, Optimized auxiliary basis sets for explicitly correlated methods, J. Chem. Phys. 129 (2008) 184108. https://doi.org/10.1063/1.3009271

[64] G. Pitsevich, A. Malevich, I. Doroshenko, Explicitly correlated study of the torsional vibrations of HSOSH molecule. Comparison with MP2/CBS(T,Q) level of theory, Mol. Cryst. Liq. Cryst., 749 (2022) 9-17. https://doi.org/10.1080/15421406.2022.2067670

[65] G.A. Pitsevich, A.E. Malevich, U.V. Lazicki, U.U. Sapeshka, The torsional states of methyl hydroperoxide molecule calculated using anharmonic zero point vibrational energy, J. Belarus. State Univ. Phys. 2 (2021) 15-24. https://doi.org/10.33581/2520-2243-2021-2-15-24

[66] D.E. Woon, T.H. Dunning, Jr., Gaussian basis sets for use in correlated molecular calculations. IV. Calculation of static electrical response properties, J. Chem. Phys., 100 (1994) 2975-2988. https://doi.org/10.1063/1.466439

[67] G.A. Pitsevich, A.E. Malevich, E.U. Sleptsov, V.V. Sapeshko, Non-empirical anharmonic analysis of vibrational states of BF_3 and BH_3 using symmetry coordinates, J. Appl. Spectrosc. 82 (2015) 46-52. https://doi.org/10.1007/s10812-015-0062-7

[68] G. Pitsevich, V. Balevicius, Hydrogen bonded pyridine *N*-oxide/trichloroacetic acid complex in polar media: 2D potential energy surface and O–H···O vibration analysis using exact vibrational Hamiltonian, J. Mol. Struct. 1072 (2014) 38-44. https://doi.org/10.1016/j.molstruc.2014.02.016

[69] D.O. Harris, G.G. Engerholm, W.D. Gwinn, Calculation of matrix elements for one-dimensional quantum-mechanical problems and the application to anharmonic oscillators, J. Chem. Phys. 43 (1965) 1515–1517. https://doi.org/10.1063/1.1696963

[70] A.S. Dickinson, P.R. Certain, Calculation of matrix elements for one-dimensional quantum-mechanical problems, J. Chem. Phys. 49 (1968) 4209-4211. https://doi.org/10.1063/1.1670738

[71] R. Meyer, Trigonometric interpolation method for one-dimensional quantum-mechanical problems, J. Chem. Phys. 52 (1970) 2053-2059. https://doi.org/10.1063/1.1673259

[72] J.C. Light, I.P. Hamilton, J.V. Lill, Generalized discrete variable approximation in quantum mechanics, J. Chem. Phys. 82 (1985) 1400-1409. https://doi.org/10.1063/1.448462

[73] D.T. Colbert, W.H. Miller, A novel discrete variable representation for quantum mechanical reactive scattering via the *S*-matrix Kohn method, J. Chem. Phys. 96 (1992) 1982-1991. https://doi.org/10.1063/1.462100

[74] G.A. Pitsevich, A.E. Malevich, Comparison of the Fourier and discrete-variable-representation methods in the numerical solution of multidimensional Schrödinger equations, J. Appl. Spectrosc. 82 (2016) 893-900. https://doi.org/10.1007/s10812-016-0200-x

[75] Mathematica, Wolfram Research, Inc. http://www.wolfram.com/mathematica

[76] G. Pitsevich, A. Malevich, Torsional motions of the free and H-bonded hydroxyl groups of the catechol molecule, J. Mol. Spectrosc. 387 (2022) 111664. https://doi.org/10.1016/j.jms.2022.111664

[77] G.A. Pitsevich, A.E. Malevich, D.G. Kisuryna, A.A. Ostyakov, U.U. Sapeshka, Torsional states and tunneling probability in HOSOH, DOSOD, and DOSOH molecules analyzed at the CBS limit, J. Phys. Chem. A 124 (2020) 8733-8743. https://doi.org/10.1021/acs.jpca.0c06411

[78] G.A. Pitsevich, A.E. Malevich, F.V. Markovich, U.U. Sapeshka, Barriers to internal rotation and tunnelling splittings of the torsional states in the $HO(CH_2)OH$, $DO(CH_2)OH$ and $DO(CH_2)OD$ molecules, Mol. Phys. 118 (2020) e1746425. https://doi.org/10.1080/00268976.2020.1746425

[79] D.-J. Liu, N.N. Haese, T. Oka, Infrared spectrum of the ν_2 vibration-inversion band of H_3O^+, J. Chem. Phys. 82 (1985) 5368-5372. https://doi.org/10.1063/1.448620

[80] J. Tang, T. Oka, Infrared spectroscopy of H_3O^+: The ν_1 fundamental band, J. Mol. Spectrosc. 196 (1999) 120-130. https://doi.org/10.1006/jmsp.1999.7844

[81] P.B. Davies, S.A. Johnson, P.A. Hamilton, T.J. Sears, Infrared diode laser spectroscopy of the $\nu_2(2^+ \leftarrow 1^-)$ band of H_3O^+, Chem. Phys. 108 (1986) 335-341. https://doi.org/10.1016/0301-0104(86)80100-8

[82] M. Araki, H. Ozeki, S. Saito, Experimental determination of the ground-state inversion splitting in D_3O^+ by microwave spectroscopy, J. Chem. Phys. 109 (1998) 5707-5709. https://doi.org/10.1063/1.477191

[83] H. Petek, D.J. Nesbitt, J.C. Owrutsky, C.S. Gudeman, X. Yang, D.O. Harris, C.B. Moore, R.J. Saykally, A study of the structure and dynamics of the hydronium ion by high resolution infrared laser spectroscopy. III. The ν_3 band of D_3O^+, J. Chem. Phys. 92 (1990) 3257-3260. https://doi.org/10.1063/1.457884